

## Thermodynamic and kinetic study of the improvement of the adsorption efficiency of Hexavalent chromium (VI) ions by encapsulated modified prickly pear peel

H. Fodil Cherif <sup>\*1</sup>, Z. Benmaamar<sup>1</sup>, O. Benkortbi<sup>2</sup>

<sup>1</sup>Fundamental and Applied Physics Laboratory, University of Blida1, Soumaa, 09000 Blida, Algeria

<sup>2</sup>Biomaterials and Transport Phenomena Laboratory, University of Dr Yahia Fares, Aind'hab, 26 000 Medea, Algeria

\* Corresponding author: h.fodilcherif@ensh.dz ; +213658367037

### ARTICLE INFO

#### Article History :

Received : 25/04/2021

Accepted : 05/05/2022

#### Key Words:

hexavalent chromium (VI);  
Prickly Pear Peel; calcium  
alginate; adsorption.

### ABSTRACT/RESUME

**Abstract:** Selected biosorbents, Prickly Pear Peels (PPP), that have been chemically activated by  $ZnCl_2$  and encapsulated in calcium alginate beads, bear the hybrid biosorbent names CA-ZnPPP, and are used for the disposal of Cr (VI) with water-based solutions. CA-ZnPPP is characterized by FT-IR spectroscopy, and Scanning electron microscopy (SEM), subsequently Batch tests were undertaken to evaluate the impact of the variables, in particular the pH value in the first instance, the retention time, and the metal content in the course of adsorption. Langmuir's isothermal model showed the greatest consistency with the test results and the biosorption rate of the single layer was  $16.28 \text{ mg g}^{-1}$  in less than 120 min working with  $1.0 \text{ g L}^{-1}$  of CA-ZnPPP, and a pH of 2. The pseudo-second order kinetic pattern correctly defined the results of the adsorption dynamics. Thermodynamic parameters ( $\Delta G^\circ$ ,  $\Delta H^\circ$ , and  $\Delta S^\circ$ ) in a temperature range of 298–328 K, have revealed that biosorption is exothermic and instantaneous. These values show that CA-ZnPPP is a favorable adsorption material for the removal of Cr (VI) in wastewater.

### I. Introduction

Numerous plant based lignocellulosic biomasses have been reported for their biosorption of Cr(VI) ions from their aqueous streams; foxtail millet shell, sugarcane bagasse, ficus auriculata leaves, olive pits [1-4], due to their accessibility, reusability and degradability. However, several studies have shown that chemical activation is a treatment performed on raw biosorbents in order to increase both their specific surface and their adsorption rate [5,7]. Nevertheless, it is essential to point out some issues related to the use of these materials. Such as the regeneration problems, and the quantities of powder recovered after an adsorption test. Indeed in the last decade, scientific research has focused on the development of new adsorbent materials aimed at avoiding the disadvantages of these conventional

materials. Therefore, the encapsulation of these materials in a polymeric matrix, i.e., chitosan [8,9] cellulose [10,11] or alginate [12,13] has been a technique used by several authors to solve the problems mentioned above. In this study, sodium alginate was chosen with regards to its numerous advantages, such as its simplicity, its biocompatibility and its low cost [14,15] compared to other encapsulating agents.

The final sorbent with the associated properties of the biopolymer and a biomaterial can behave the same way as a traditional ion exchange or chelating resin [16]. In the present work, an attempt has been made to investigate the adsorption potential of activated Prickly Pear Peels by Zinc chloride ( $ZnCl_2$ ) and immobilization in calcium alginate, for the removal of hexavalent chromium Cr (VI).

## II. Materials and methods

### II.1. Preparation of Synthetic solution

A primary solution of 1000 mg.L<sup>-1</sup> potassium chromate was prepared by dissolving 3,74 g K<sub>2</sub>CrO<sub>4</sub> in 1000ml of distilled water. Working solutions of concentration 10-100 mg.L<sup>-1</sup> were made by adequately diluting a stock solution in distilled water.

### II.2. Preparation of activated carbon

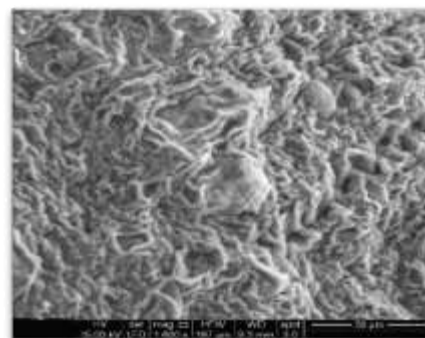
PPP were air-dried and pulverized to pass through a 100 mesh sieve, then immersed in a 5 mol.L<sup>-1</sup> ZnCl<sub>2</sub> solution for 24 h, and dried at 378 K. Finally the pretreated sludge was calcined at 973K for 2h with a heating rate of 5 °C.min<sup>-1</sup>, and then cooled to room temperature. Subsequently, the sample was washed with 2 mol.L<sup>-1</sup>HCl, until the pH changed to 7,0, dried at 378 K, then sealed and stored.

### II.3. Beads formation

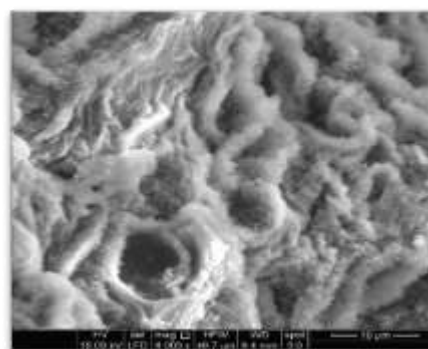
A 2% (W/W) sodium alginate gel was prepared by dissolving the sodium salt in 96ml of hot distilled water, the required amount of activated biosorbent (Zn-PPP) powder (2g) was added into the cooled alginate gel. The homogenized product, composed of sodium alginate and biosorbent, was poured drop by drop into 200 mL of 0,1 M CaCl<sub>2</sub>. The beads obtained are kept under agitation for 24 hours, then rinsed several times with distilled water. The biosorbent obtained is named CA-ZnPPP.

### II.4. Characterization of the adsorbent

The Scanning electron microscope (SEM) technique was used to examine the surface physical morphology of the adsorbent. As represented in Figure 1(a,b), the surface of CA-ZnPPP is full of cavities and comparatively irregular as a result of activation and the pores were of different sizes and shapes, which contributes to the high surface area and Cr(VI) adsorption properties of CA-ZnPPP. The FT-IR spectra of the CA-ZnPPP were used to identify functional groups present on the adsorbents and the result was indicated in Figure 2. The FT-IR spectra of adsorbent are measured in the range of 400-4000 cm<sup>-1</sup>. In Fig 2, the strong adsorption band at 3347,61 cm<sup>-1</sup> corresponds to the O-H stretching vibration of alcohol, phenol or carboxylic acid. The small peak at 2924,17 cm<sup>-1</sup> indicates the presence of a C-H stretching vibration in the methyl group. The peaks at 1589,39 and 1410,17 cm<sup>-1</sup> are an identification of COO, C=O groups. 1024,13 cm<sup>-1</sup> is the stretching vibration of C-O-C, -CH<sub>3</sub>. The acidic groups are protonated at pH 2.0, which accounts for the effective adsorption of hexavalent chromium ions on the activated biosorbent [17].



(a)



(b)

Figure 1 (a,b). Scanning electron microscopy of CA-ZnPPP

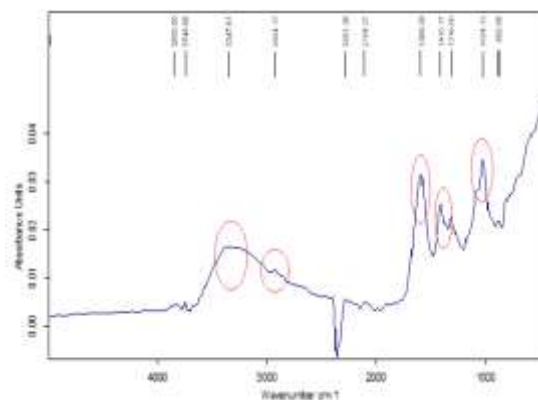


Figure 2. The FT-IR Spectra of CA-ZnPPP

### II.5. Adsorption Studies

Adsorption kinetics of hexavalent chromium Cr(VI) onto CA-ZnPPP were carried out under the effect of two important variables: pH and retention time. All tests were undertaken by adding 0,1 g of adsorbent into 100 mL of Cr(VI) solution (10 mg.L<sup>-1</sup>). The solution's pH was adjusted by 0.1 mol.L<sup>-1</sup> NaOH or 0.1 mol.L<sup>-1</sup> HCl. The sample was agitated at 150 rpm. The considered concentration of Cr(VI) was obtained at  $\lambda_{max} = 540 \text{ nm}$  (by UV-1700 Pharma Spec Shimadzu spectrophotometer) after complexation with 1,5-diphenylcarbazide. [18]

The adsorbed amount of Cr(VI),  $q$  (mg/g), (Eq. (1)) was calculated as:

$$q = \frac{(C_0 - C_t)V}{m} \quad (1)$$

where  $C_0$  (mg/L) is the starting Cr(VI) content,  $C_t$  (mg/L) is the Cr(VI) content at the present moment  $t$ ,  $V$  (L) is the volume of chromium solution, and  $m$  (g) is the weight in grams of the materials used for adsorption.

### III. Results and discussion

#### III. 1. Influence of time

The influence of the treatment time on the reduction of Cr (VI) in solution was analyzed at a different time (0–180 min) with an initial concentration of Cr(VI)  $10 \text{ mg}\cdot\text{L}^{-1}$ . In accordance with Figure 3. The retention ability moved quickly during the initial 10 min and then slowly increased again until an unchanged result was obtained when the availability site became saturated. The retention ability was  $8,6 \text{ mg}\cdot\text{g}^{-1}$  at 120 min.

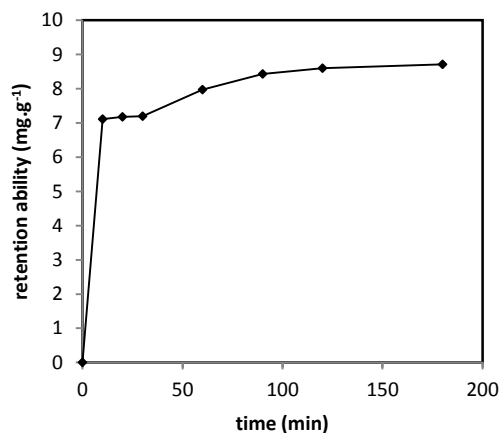
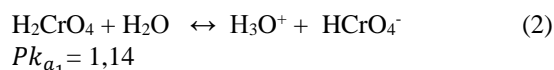


Figure 3. Influence of time on equilibrium adsorption of PPP

#### III. 2. Influence of the pH

The initial pH of the solution is a very important parameter, its variation may change the different forms in which hexavalent chromium can exist in a solution ( $\text{HCrO}_4^-$  and  $\text{CrO}_4^{2-}$ ); These are obtained from the dissociation of chromic acid in water, according to the following equations: [19]



$$P_{k_{a_2}} = 6,34$$

At a  $\text{pH} < 2$ ,  $\text{HCrO}_4^-$  is the predominant form. In the pH band of 2-6, various chromium ions such as  $\text{HCrO}_4^-$ ,  $\text{CrO}_4^{2-}$  and  $\text{Cr}_2\text{O}_7^{2-}$  can reside together, principally in the form of  $\text{HCrO}_4^-$ . At a  $\text{pH} > 7,5$ ,  $\text{CrO}_4^{2-}$  is the exclusive chromate form [20].

The pH level can also affect the adsorption capacity of the adsorbent; This can lead to the variation of the charge on the surface of the adsorbent, as well as the degree of the protonation of its functional groups [21]. The pH of zero charge point ( $\text{pH}_{\text{PZC}}$ ) is the pH at which the surface of the adsorbent is neutral [22]; An understanding of the latter, allows us to know which pH will positively or negatively charge the adsorbent [23]. For a pH higher than  $\text{pH}_{\text{PZC}}$ , the adsorbent presents a predominance of negative charges and conversely for a pH below the isoelectric point. In our case the determination of the isoelectric point for our adsorbent, as can be seen in figure 4, allows us to deduce that it is positively charged as the  $\text{pH}_{\text{PZC}}$  was found to be equal to 7.5.

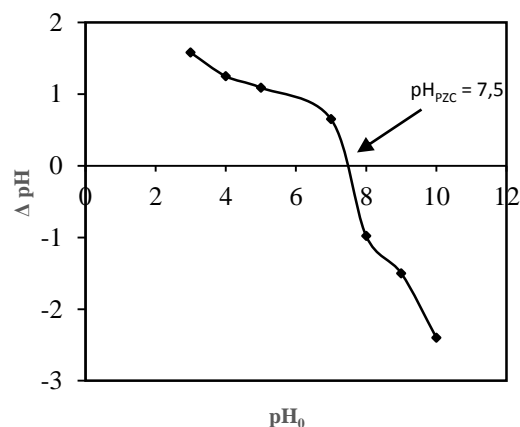


Figure 4. Determination of point of Zero charge ( $\text{pH}_{\text{PZC}}$ ) of CA-ZnPPP

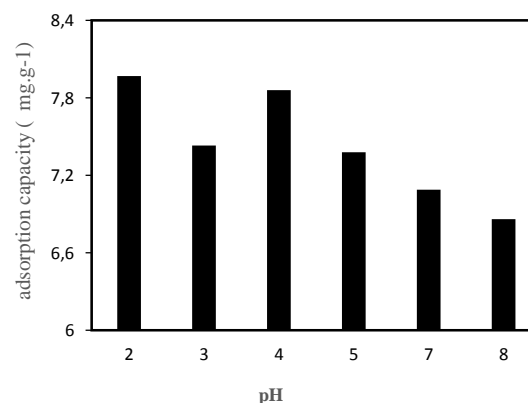


Figure 5. Effect of pH on Cr(VI) adsorption capacity

According to figure 5 , we note that the rate of elimination decreases with an increasing pH, a maximum is reached at pH=2, therefore, at a lower pH, adsorption is enhanced by the electrostatic attraction between the protonated material surface and the negatively charged chromate ions in the solution.

**III. 3. Adsorption Isotherm studies**

For a greater clarity of the adsorption phenomenon, isothermal research is very decisive. Langmuir and Freundlich isotherms were commonly used in recent research to give an explanation of the interaction of adsorbents. The Freundlich model assumes a non-homogeneous adsorption surface and active sites of different energy : [24]

$$q_e = K_F C_e^{1/n} \tag{4}$$

The equation could be reconfigured into a linear expression as follows:

$$\text{Log } q_e = \text{log } K_F + \frac{1}{n} \text{log } C_e \tag{5}$$

where  $q_e$  ( $\text{mg} \cdot \text{g}^{-1}$ ) is the amount of Cr (VI) adsorbed per unit of adsorbent at a steady-state ,  $C_e$  ( $\text{mg} \cdot \text{L}^{-1}$ ) is the residual strength of Cr (VI) in the solution after adsorbing at equilibrium,  $K_F$  and  $n$  are the Freundlich adsorption isotherm constants which indicate the extent of the adsorption and the degree of nonlinearity between the concentration and the adsorption respectively [25,26] . The value of  $1/n$ , which is generally in the range of 0 and 1, illustrates the consequences of concentration on adsorption efficiency . The coefficients of  $K_F$  and  $1/n$  can be calculated from the line interception and the incline of the flat line between  $\text{log } c_e$  and  $\text{log } q_e$  .

Langmuir's theory focuses on the precept that sorption takes place at precise and uniform locations in the sorption material. It can be formulated in a non-linear form [27]

$$q_e = \frac{q_m K_L C_e}{1 + K_L C_e} \tag{6}$$

The equation can be linearized as follows:

$$\frac{C_e}{q_e} = \frac{C_e}{q_m} + \frac{1}{K_L q_m} \tag{7}$$

Where  $q_m$  ( $\text{mg } \text{g}^{-1}$ ) is the maximum amount of monolayer adsorption on the area of the adsorbent [28], and  $K_L$  ( $\text{L} \cdot \text{mg}^{-1}$ ) is Langmuir's invariable linked to the power adsorption . It should be pointed out that the major particularities of the Langmuir isotherm can be expressed in terms of a dimensionless,  $R_L$  (equilibrium parameter), as given in the equation:

$$R_L = \frac{1}{1 + K_L C_0} \tag{8}$$

where  $K_L$  is the Langmuir's invariable,  $c_0$  ( $\text{mg } \text{L}^{-1}$ ) is the initial Cr (VI) concentration. The values of  $R_L$  indicate the isothermal structure :  $R_L > 1$  (unfavourable),  $R_L = 1$  (linear),  $1 > R_L > 0$  (favourable), and  $R_L = 0$  (irreversible). The Langmuir and Freundlich isotherms plotted for Cr(VI) adsorption on CA-ZnPPP are shown in Fig.6, Fig.7 respectively ; and the values of the constants and the correlation coefficients of all the types of both of the models are described in Table 1.

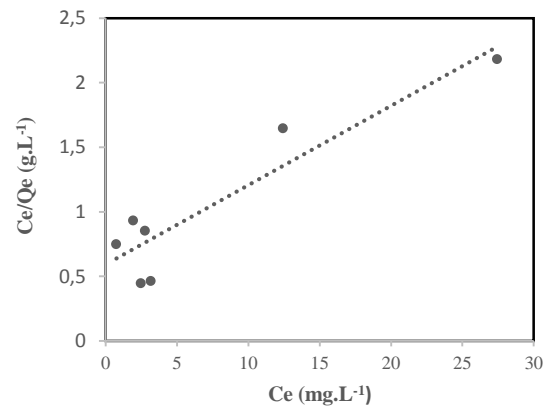


**Figure 6 . Langmuir isotherm plot for the adsorption of Cr(VI) onto CA-ZnPPP.**

**Table 1.** Adsorption Isotherm constants and correlation coefficients.

Langmuir model		Freundlich model	
$Q_{max}$ ( $\text{mg } \text{g}^{-1}$ )	16.28	$K_F$ ( $\text{mg } \text{g}^{-1}$ ) ( $\text{L } \text{g}^{-1}$ ) <sup>1/n</sup>	1.98
$K_L$ ( $\text{L } \text{mg}^{-1}$ )	0.103	$1/n$	0.59
$R^2$	0.85	$R^2$	0.79

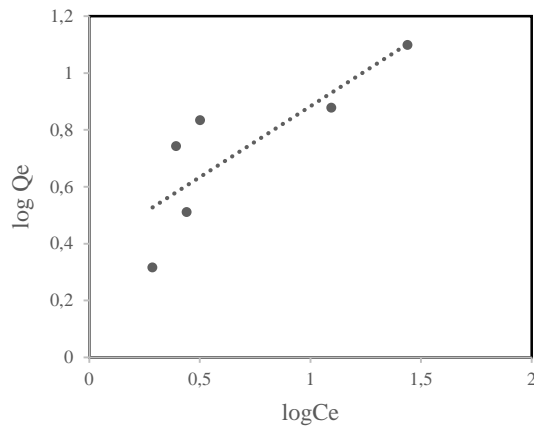


**Figure 7.** Freundlich isotherm plot for the adsorption of Cr(VI) onto CA-ZnPPP.

The data obtained experimentally was found to fit best with the Langmuir isotherm model with a regression coefficient of ( $R^2$ ) 0.85, which indicates the monolayer adsorption of Cr(VI) onto CA-ZnPPP. The value of  $R_L$  (0.492) also supports the feasibility of this isotherm, which demonstrates that the configuration of the isothermal system must be appropriate ( $0 < R_L < 1$ ) [29]

### III.4. Kinetic Studies

The study of kinetics is an important part of adsorption research as it explains the rate of adsorption from which the mechanisms of the process and the rate-controlling steps can be predicted. In this report, various modes of predicting adsorption kinetics of Cr (VI) onto CA-ZnPPP were used (pseudo-first order, pseudo-second order, and intra-particle diffusion model).

**Pseudo-first-order model.** The differential variant of the pseudo-first-order rate equation, which is frequently used in the case of the surface concentration of an adsorbate obtained from an aqueous solution, is indicated as below [26].

$$\frac{dq_t}{dt} = K_1 (q_e - q_t) \quad (9)$$

When  $q_t = 0$  at  $t = 0$  and  $q_t = q_t$  at  $t = t$ , equation (9) can be inserted into the equation below

$$\ln(q_e - q_t) = \ln q_e - K_1 t \quad (10)$$

Where  $q_t$  ( $\text{mg g}^{-1}$ ) is the adsorption amount of hexavalent chromium Cr (VI) per unit of adsorbent at time  $t$ ,  $k_1$  ( $\text{min}^{-1}$ ) is the pseudo-first-order yield parameter, and  $t$  (min) is the adsorption time. The adsorption yield parameter ( $k_1$ ) can be measured from the plot of  $\ln(q_e - q_t)$  against  $t$ .

**Pseudo-second-order model.** The pseudo-second-order expression is as described in the following equation [30]:

$$\frac{dq_t}{dt} = K_2 (q_e - q_t)^2 \quad (11)$$

By integrating Eq. 11 for the limit condition  $t = 0$  to  $t = t$  and  $q_t = 0$  and  $q_t = q_t$ , the resulting equation can actually be rearranged in a linear form:

$$\frac{t}{q_t} = \frac{1}{K_2 q_e^2} + \frac{t}{q_e} \quad (12)$$

Where  $k_2$  ( $\text{g mg}^{-1} \text{min}^{-1}$ ) is the pseudo-second-order yield parameter. In general, the constant  $k_2$  is also applied to measure the original degree of adsorption  $h$  ( $\text{mg g}^{-1} \text{min}^{-1}$ ) as shown [25]:

$$h = \lim_{t \rightarrow 0} (K_2 q_e^2) \quad (13)$$

**Intra-particle diffusion model.** The Intra-particle diffusion model is frequently applied to establish the adsorption process for design purposes. It can be represented by the equity equation [26]:

$$q_t = K_i t^{(1/2)} + I \quad (14)$$

Where  $k_i$  ( $\text{mg g}^{-1} \text{min}^{-1/2}$ ) is the intra-particle diffusion yield parameter.

The amount of  $I$  represents the depth of the separating layer [26].

The parameters of  $h$ ,  $k_2$ , and  $q_e$  may be estimated using the plot of  $t/q_t$  vs  $t$ .

**Table 2.** Kinetics parameters

$Q_m(\text{exp})$	Pseudo-first order		Pseudo –second order		Intra-particle diffusion model	
	$K_1$		$K_2$		$K_i$	$R^2$
8,68		2.37		0.021	0,1864	0,93
	$Q_e$	8.42	$q_e$	8.93		
	$R^2$	0.67	$R^2$	0,99		

The parameters of all the models involved in the measurement of kinetic adsorption are summarized in the Table 2. The linking factors  $R^2$  for the pseudo-second order model ( $R^2 = 0.999$ ) were higher than the values of the intra-particle diffusion factors ( $R^2 = 0.921$ ), which suggest a chemistry-sorption mechanism [31].

**III.5. Thermodynamic studies**

In order to check whether the biosorption process occurs instantaneously, Gibbs free energy and entropy coefficients were taken into account. By plotting  $\ln K$  vs  $1/T$  (Fig. 8), the change in Free energy of Gibbs ( $\Delta G^\circ$ ), enthalpy ( $\Delta H^\circ$ ), and entropy ( $\Delta S^\circ$ ) for the biosorption mechanisms, were identified using Eqs. (15) and (16).

$$\Delta G^\circ = -RT \ln K \tag{15}$$

Where  $\Delta G^\circ$  is Free energy of Gibbs ( $\text{kJ mol}^{-1}$ ),  $R$  is the global gas factor ( $8.314 \text{ J mol}^{-1} \text{ K}^{-1}$ ),  $T$  is the total temperature (K), and  $K$  is the balance constant ( $c_s/c_e$ ).  $c_s$  is the Cr(VI) concentration on adsorbent ( $\text{mg L}^{-1}$ ) and  $c_e$  is the balance concentration of hexavalent chromium Cr(VI) ions ( $\text{mg L}^{-1}$ ). The enthalpy ( $\Delta H$ ) and entropy ( $\Delta S$ ) values can be deduced by using Van't Hoff relation :

$$\ln K = \frac{\Delta S^\circ}{R} - \frac{\Delta H^\circ}{RT} \tag{16}$$

The enthalpy and entropy values of Cr (VI) were resulting directly from the gradient of ( $\Delta H/R$ ) and intercept ( $\Delta S/R$ ). From Table 3, free energy of Gibbs,  $\Delta G$  turns to  $-3.48 \text{ kJ mol}^{-1}$  at 298 K, which indicates a favourable biosorption process that was spontaneous and exothermic ( $\Delta H = -23.83 \text{ kJ mol}^{-1}$ ) over the temperature range of 298 to 328 K.

It reveals a favourable biosorption process, spontaneous and exothermic, beyond the temperature limits of 298 to 328 K. The negative entropy change within the same temperature range ( $\Delta S = -68.26 \text{ J mol}^{-1} \text{ K}^{-1}$ ) reveals a rise in the unpredictability of the solid-liquid interface and the naturalness of adsorption [32].

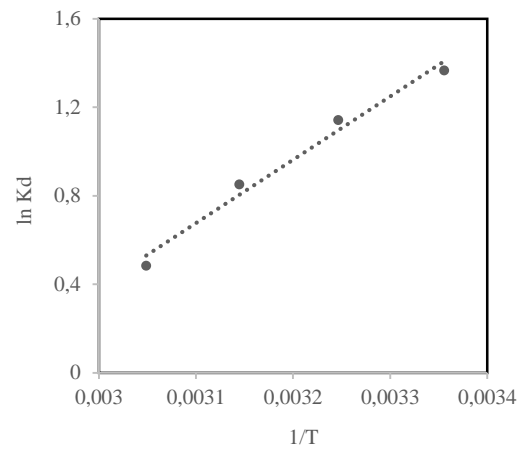


Figure 8. Van't Hoff graphic

Table 3. The data of the thermodynamic variables for Cr(VI) adsorption on CA-ZnPPP

$\Delta G^\circ$ (KJ/mol)		$\Delta H^\circ$ (K J.mol <sup>-1</sup> )	$\Delta S^\circ$ (J.mol <sup>-1</sup> )	$R^2$
298 K	-3.48			
308 K	-2.8	-23,83	-68,26	0,98
318K	-2.12			
328 K	-1.44			

**IV. Conclusion**

In this work, immobilized and activated PPP was used effectively as a composite adsorbent for the abatement of hexavalent chromium (Cr VI). In batch mode, adsorption strongly depended on two working parameters (pH, contact time). The results indicated the following optimal conditions; a pH value of 2 and 120 min of retention time. The biosorption ability was of  $16,28 \text{ mg.g}^{-1}$ , as a function of the Langmuir model. Thermodynamics studies show that the biosorption mechanisms are favourable and spontaneous with the highest adsorption capability capped at 298 K, and heating is not required to promote its adsorption capacity. Kinetics

surveys have revealed that the adsorption scheme of Cr (VI) followed the pseudo-second order pattern, provides the best correlation coefficient. CA-ZnPPP could be a great alternative for efficient disposal and remediation of hexavalent chromium sorts from aqua.

**V. References**

- Peng, S.H.; Wang, R.; Yang, L.Z.; He, L.; He, X.; Liu, X. Biosorption of copper, zinc, cadmium and chromium ions from aqueous solution by natural foxtail millet shell. *Ecotoxicology and Environmental Safety* 165 (2018) 61-69.

2. Ullah, I.; Nadeem, R.; Iqbal, M.; Manzoor, Q. Biosorption of chromium onto native and immobilized sugar cane bagasse waste biomass. *Journal of Ecological Engineering* 60 (2013)99-107.
3. Rangabhashiyam, S.; Suganya, E.; Lity, A.V.; Selvaraju, N. Equilibrium and kinetics studies of hexavalent chromium biosorption on a novel green macroalgae *Enteromorpha* sp. *Research on chemical Intermediates* 42 (2016) 1275-1294.
4. Martín-Lara, M.A.; Blázquez, G.; Trujillo, M.C.; Pérez, A.; Calero, M. New treatment of real electroplating wastewater containing heavy metal ions by adsorption onto olive stone. *Journal of Cleaner Production* 81 (2014) 120-129.
5. Ali, I.H.; Alrafai, H.A. Kinetic, isotherm and thermodynamic studies on biosorption of chromium(VI) by using activated carbon from leaves of *Ficus nitida*. *Chemistry Central Journal* 10(2016) 36.
6. Enniya, I.; Rghioui, L.; Jourani, A. Adsorption of hexavalent chromium in aqueous solution on activated carbon prepared from apple peels. *Sustainable Chemistry and Pharmacy* 7(2018) 9–16.
7. Rangabhashiyam, S.; Selvaraju, N. Adsorptive remediation of hexavalent chromium from synthetic wastewater by a natural and ZnCl<sub>2</sub> activated *Sterculiaguttata* shell. *Journal of Molecular Liquids* 207(2015) 39–49.
8. Dandil, S.; Akin Sahbaz, D.; Acikgoz, C. Adsorption of Cu(II) ions onto crosslinked chitosan/Waste Active Sludge Char (WASC) beads: kinetic, equilibrium, and thermodynamic study. *International Journal of Biological Macromolecules* 136 (2019) 668–675.
9. Le, T.T.N.; Le, V.T.; Dao, M.U.; Nguyen, Q.V.; Vu, T.T.; Nguyen, M.H.; Tran, D.L.; Le, H.S. Preparation of magnetic graphene oxide/chitosan composite beads for effective removal of heavy metals and dyes from aqueous solutions. *Chemical Engineering Communications* 206 (2019) 1337–1352.
10. Pan, Y.; Xie, H.; Liu, H.; Cai, P.; Xiao, H. Novel cellulose/montmorillonite mesoporous composite beads for dye removal in single and binary systems. *Bioresource Technology* 286 (2019) 121366.
11. Xie, H.; Pan, Y.; Xiao, H.; Liu, H. Preparation and characterization of amphoteric cellulose–montmorillonite composite beads with a controllable porous structure. *Journal of Applied Polymer Science* 136 (2019) 47941.
12. Dominguez, M.A.; Etcheverry, M.; Zanini, G.P. Evaluation of the adsorption kinetics of brilliant green dye onto a montmorillonite/alginate composite beads by the shrinking core model. *Adsorption* 25 (2019) 1387–1396.
13. Biswas, S.; Sen, T.K.; Yeneneh, A.M.; Meikap, B.C. Synthesis and characterization of a novel Ca-alginate-biochar composite as efficient zinc (Zn<sup>2+</sup>) adsorbent: thermodynamics, process design, mass transfer and isotherm modeling. *Separation Science and Technology* 54(2019)1106–1124.
14. Kurczewska, J.; Ceglowski, M.; Schroeder, G. Alginate/PAMAM dendrimer – halloysitebeads for removal of cationic and anionic dyes. *International Journal of Biological Macromolecules* 123 (2019)398–408.
15. Fiol, N.; Poch, J.; Villaescusa, I. Grape stalks wastes encapsulated in calcium alginate beads for Cr(VI) removal from aqueous solutions. *Separation Science and Technology* 40 (2005)1013–1028.
16. Bajpai, S.K.; Sharma, S. Investigation of swelling/degradation behaviour of alginate beads cross linked with Ca<sup>2+</sup> and Ba<sup>2+</sup> ions. *Reactive and Functional Polymers* 59 (2004) 129–140.
17. Rangabhashiyam, S.; Selvaraju, N. Adsorptive remediation of hexavalent chromium from Synthetic wastewater by a natural and ZnCl<sub>2</sub> activated *Sterculiaguttata* shell. *Journal of Molecular Liquids* 207(2015)39-49.
18. Eaton, A.D.; Clesceri, L.S.; Greenberg, A.E. Standard Methods for the Examination of water and waste water. *American Public Health Association* (1995) 4-23.
19. Lazaridis, N. K.; Charalambous, C. Sorptive removal of trivalent and hexavalent chromium from binary aqueous solutions by composite alginate-geothite beads. *Water Research* 39 (2005) 4385–4396.
20. Rodrigues, L. A.; Sakane, K. K.; Simonetti, E. A. N.; Thim, G. P. Cr total removal in aqueous solution by PHENOTAN AP based tannin gel (TFC). *Journal of Environmental Chemical engineering* 3(2015) 725–733.
21. Tan, X.; Gao, B.; Xu, X.; Wang, Y.; Ling, J.; Yue, Q.; Li, Q. Perchlorate uptake by wheat straw based adsorbent from aqueous solution and its subsequent biological regeneration. *Chemical Engineering Journal* 211-212 (2012) 37-45.
22. Talreja, N.; Kumar, D.; Verma, N. Removal of hexavalent chromium from water using Fegrown carbon nanofibers containing porous carbon microbeads. *Journal of Water Process Engineering* 3 (2014) 34-45.
23. Čerović, Lj.S.; Milonjić, S.K.; Todorović, M.B.; Trtanj, M.I.; Pogozhev, Y.S.; Blagoveschenskii, Y.; Levashov, E.A. Point of zero charge of different carbides. *Colloids and Surfaces A: Physicochemical and Engineering Aspects* 297 (2007) 1-6.
24. Gupta, N.; Kushwaha, A. K.; Chattopadhyaya, M. C. Application of potato (*Solanum tuberosum*) plant wastes for the removal of methylene blue and malachite green dye from aqueous solution. *Arabian Journal of Chemistry* 9 (2016) 707–716.
25. Sen, T. K.; Afroze, S.; Ang, H. M. Equilibrium, kinetics and mechanism of removal of methylene blue from aqueous solution by adsorption onto pine cone biomass of *Pinus radiata*. *Water air and Soil Pollution* 218 (2011) 499-515.
26. Vimonses, V.; Lei, S. M.; Jin, B.; Chow, C. W. K.; Saint, C. Kinetic study and equilibrium isotherm analysis of Congo Red adsorption by clay materials. *Chemical Engineering Journal* 148 (2009) 354–364.
27. Langmuir, I. The adsorption of gases on plane surfaces of glass, mica and platinum. *Journal of the American Chemical Society* 40 (1918) 1361–1403.
28. Srilakshmi, C.; Saraf, R. Ag-doped hydroxyapatite as efficient adsorbent for removal of Congo red dye from aqueous solution: Synthesis, kinetic and equilibrium adsorption isotherm analysis. *Microporous and Mesoporous Materials* 219 (2016) 134–144.
29. Sartape, A. S.; Mandhare, A. M.; Jadhav, V. V.; Raut, P. D.; Anuse, M. A. Removal of malachite green dye from aqueous solution with adsorption technique using *Limonia acidissima* (wood apple) shell as low cost adsorbent. *Arabian Journal of Chemistry* 10 (2017) S3229–S3238.

30. Ho, Y. S.; McKay, G. Pseudo-second order model for sorption processes. *Process Biochemistry* 34 (1999) 451–465.
31. Zhang, C. L.; Qiao, G. L.; Zhao, F.; Wang, Y. Thermodynamic and kinetic parameters of ciprofloxacin adsorption onto modified coal fly ash from aqueous solution. *Journal of Molecular Liquids* 163 (2011) 53–56.
32. Ezechi, E. H.; Kutty, S. R. M.; Malak Ahmad, A.; Isa, A. M. H. Characterization and optimization of effluent dye removal using a new low cost adsorbent: Equilibrium, kinetics and thermodynamic study. *Process Safety and Environmental Protection* 98 (2015) 16–32.

**Please cite this Article as:**

Fodil Cherif H., Benmaamar Z., Benkortbi O., Thermodynamic and Kinetic study of the improvement of the adsorption efficiency of Hexavalent chromium (VI) ions by encapsulated modified prickly pear peel, *Algerian J. Env. Sc. Technology*, 9:3 (2023) 3195-3202